

Fatigue crack propagation in cold drawn steel

J. Toribio^{a,*}, B. González^a, J.C. Matos^b

^a Department of Materials Engineering, University of Salamanca, E.P.S., Campus Viriato, Avda. Requejo 33, 49022 Zamora, Spain

^b Department of Computing Engineering, University of Salamanca, E.P.S., Campus Viriato, Avda. Requejo 33, 49022 Zamora, Spain

Received 7 April 2006; received in revised form 30 June 2006; accepted 3 July 2006

Abstract

This paper deals with the fatigue crack growth in pearlitic steel wires in the form of hot rolled bar and cold drawn wire. The progress of crack front was analysed by means of the evolution of the aspect ratio with the relative crack depth, and this latter was evaluated during the tests by a compliance method. Results show that cold drawing is beneficial from the point of view of crack growth rate, i.e., cracking is slower in the cold drawn wire (final commercial product) than in the hot rolled bar (base material). In spite of the oriented pearlitic microstructure of the cold drawn steel, fatigue crack propagation develops in mode I, i.e., cracking takes place by maintaining its original plane. A materials science reasoning is proposed to explain this behaviour on the basis of the pearlitic microstructure of the steel and the large geometry changes in the vicinity of the crack tip.

© 2007 Elsevier B.V. All rights reserved.

Keywords: Pearlitic steels; Steelmaking; Cold drawing; Strength anisotropy; Crack deflection; Crack tip blunting

1. Introduction

High-strength cold-drawn pearlitic steel is widely used in the prestressed concrete technique in the form of wires, cables and strands, and it is frequently subjected to cyclic (fatigue) loading able to produce the growth of cracks.

There are studies in the scientific literature about fatigue crack propagation in wires from the analytical-numerical [1–3] or experimental [4,5] points of view, although the fatigue phenomenon in wires is far from being totally understood.

In this paper the differences, with regard to fatigue crack growth, between a hot rolled bar and a cold drawn wire (commercial prestressing steel) are studied, since the strain hardening process to make prestressing steel produces, apart from a clear improvement of mechanical properties (the final aim of manufacturing) a change in the fatigue performance.

2. Experimental procedure

The material used was a pearlitic steel with eutectoid composition. It was analysed in two forms: firstly, as a hot rolled bar (steel E0), and secondly, as a commercial prestressing steel

wire after cold drawing the hot rolled bar in seven passes (steel E7).

The main mechanical properties of the steel are summarized in Table 1, where E is the Young's modulus, σ_Y the yield strength and σ_R the ultimate tensile strength. Their stress–strain curves are plotted in Fig. 1.

The specimens for the fatigue tests were circular rods of 11.0 and 5.1 mm diameter (respectively the hot rolled bar and the prestressing steel wire) and a mechanical notch was produced to initiate fatigue cracking. Tests were performed at room temperature, step by step under load control, the load being constant in a step and decreasing from one to another step. Samples were subjected to tensile cyclic loading with an R factor equal to zero, and a frequency of 10 Hz. The maximum load in the first loading stage corresponded to a value of about half the yield strength in the smooth wire and was reduced between 20 and 30% from one to another step (cf. Fig. 2).

The crack front was modelled as an ellipse with its centre located at the periphery of the rod (Fig. 3). It was defined from a set of real points taken from the actual crack front and using a least squares fitting technique to adjust the theoretical (modelled) crack front to the real one.

The crack length was evaluated by means of the compliance of the samples, cf. Fig. 4 showing the dimensionless compliance ($1/CED$) versus the dimensionless crack length (a/D) for both steels. The compliance (C) for each test was obtained from the

* Corresponding author. Tel.: +34 980 545000; fax: +34 980 545002.
E-mail address: toribio@usal.es (J. Toribio).

Table 1
Mechanical properties of the steels

Steel	E (GPa)	σ_Y (GPa)	σ_R (GPa)	ε_R	R_A (%)
E0	202	0.70	1.22	0.068	31.24
E7	209	1.48	1.82	0.059	23.05

ε_R : ultimate strain; R_A : reduction of area at fracture.

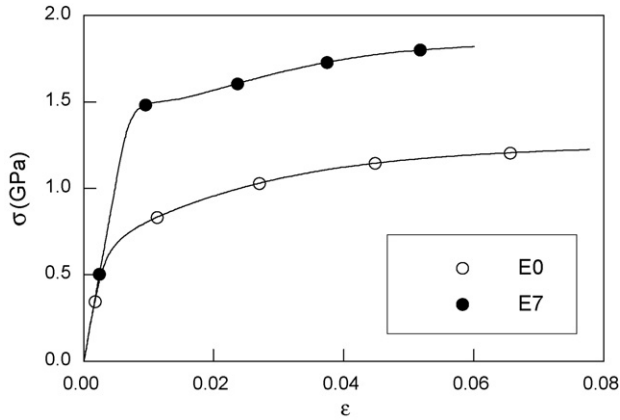


Fig. 1. Stress–strain curves of the steels.

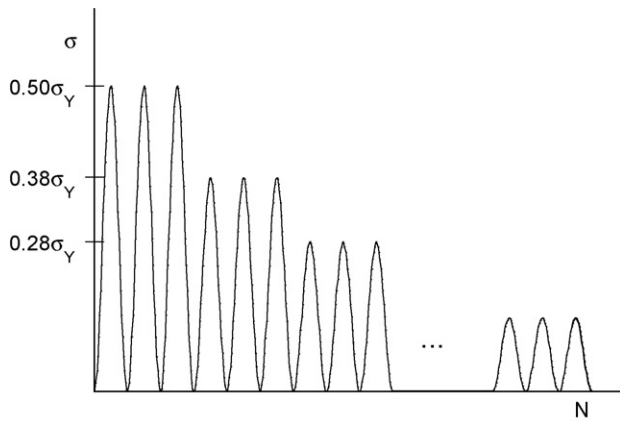


Fig. 2. Loading scheme during the tests.

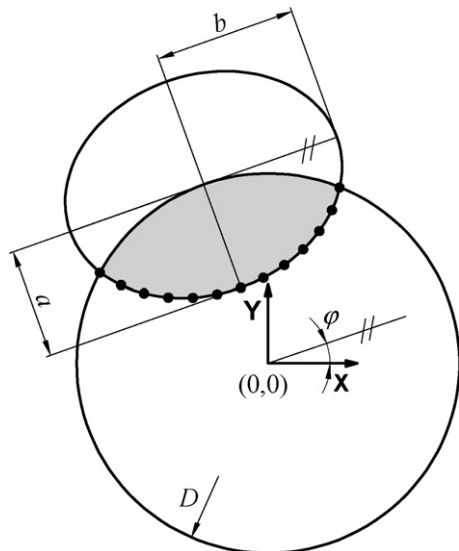


Fig. 3. Crack front modelling.

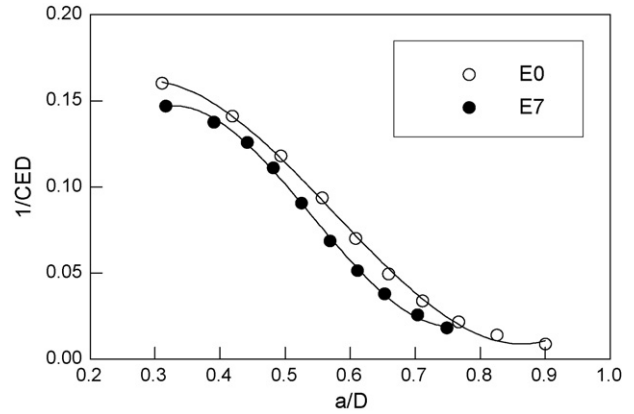


Fig. 4. Dimensionless compliance for both steels.

last loading step at which the relationship between the applied load (F , measured by means of the load cell) and the relative displacement between two reference points in the sample (u , evaluated by means of a dynamic extensometer located in front of the crack mouth) allows the computation of the compliance $C = u/F$. Finally, the compliance was related to the crack geometry (relative crack depth a/D and crack aspect ratio a/b , see Fig. 3), these geometric parameters being obtained by optical microscopy after fracture (Figs. 5 and 6).

The slight differences can be attributed to the different evolution of crack shape during fatigue in both steels, since the specimen dimensions were taken as proportional to guarantee the geometric similarity and thus a theoretically unique plot in dimensionless compliance is obtained if the same crack aspect ratio a/b is achieved.

3. Experimental results

3.1. Crack aspect evolution

In the fractographs obtained by fatigue and posterior fracture of the wires, the crack front evolution was observed during the different steps (Figs. 5 and 6). The fatigue surfaces of the hot rolled bar and the cold drawn wire are developed in mode I, although a certain 3D aspect is observed in some local areas,

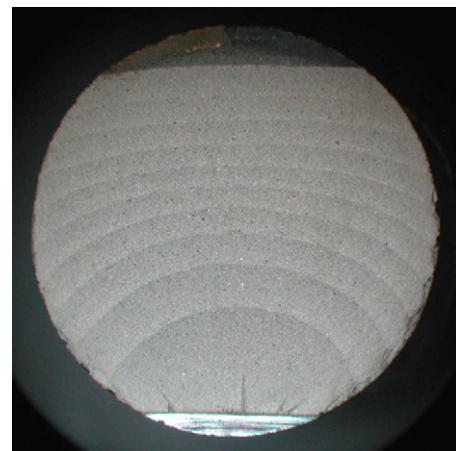


Fig. 5. Fatigue surface (hot rolled steel E0).

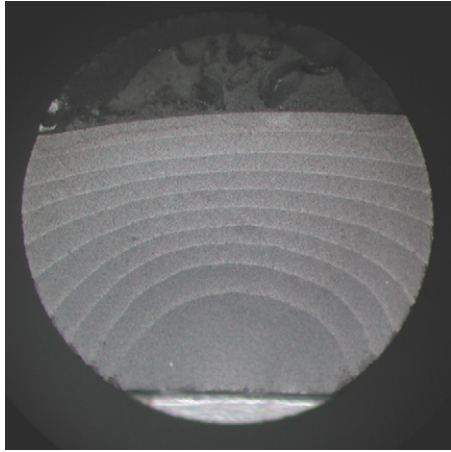


Fig. 6. Fatigue surface (cold drawn steel E7).

especially near the specimen outer surface. The fatigue surfaces of the hot rolled bar (isotropic after hot rolling and before cold drawing) exhibit a granular texture, with fatigue marks less pronounced and a more regular geometry (Fig. 5). Contrarily, in the prestressing steel wire (anisotropic after cold drawing) the fatigue surface also develops in mode I in its own plane, the beach marks being clearly detectable by visual inspection (Fig. 6), with certain irregularities during the first stages. At the specimen surface (plane stress state), some tearing zones appear, as observed in Fig. 7.

Fig. 8 plots the crack aspect ratio a/b versus the dimensionless crack length (a/D). In the first phases of the fatigue crack growth, the prestressing steel (E7) presents more curved cracks (higher a/b) than the hot rolled bar (E0), and both steels reach the same crack aspect ratio for $a/D \cong 0.4$, the trend being different at the final stages of the process.

3.2. Crack growth rate

The fatigue crack propagation was analysed by means of fatigue tests under load control, with constant stress range $\Delta\sigma$ during each step and decreasing steps (i.e., the stress range decreases from one to another step), obtaining Figs. 9 and 10,



Fig. 7. Detail of the crack at the specimen surface.

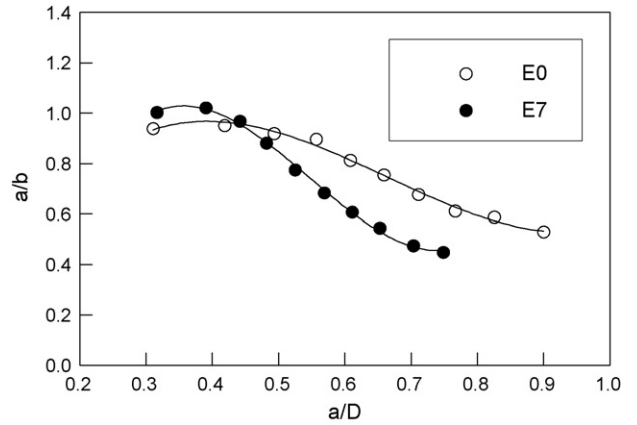


Fig. 8. Evolution of the crack aspect ratio a/b in the hot rolled steel (E0) and the cold drawn wire (E7).

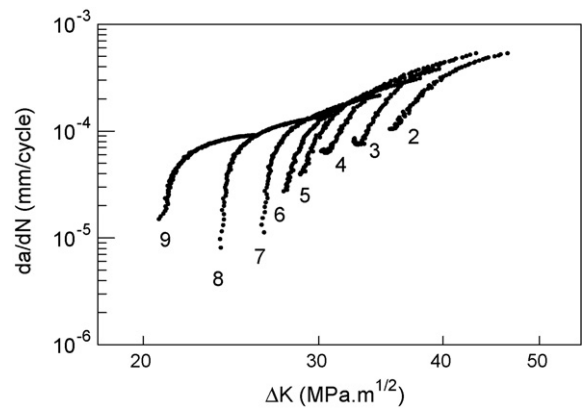


Fig. 9. Fatigue crack growth laws (hot rolled steel E0). The number next to each branch of the curve indicates the fatigue step associated with it.

where da/dN is the cyclic crack growth by fatigue and ΔK the stress intensity range, both variables being related by the equation:

$$\Delta K = Y\Delta\sigma\sqrt{\pi a} \tag{1}$$

The dimensionless stress intensity factor Y for the geometry under consideration (cracked wire) was calculated by Astiz [6]

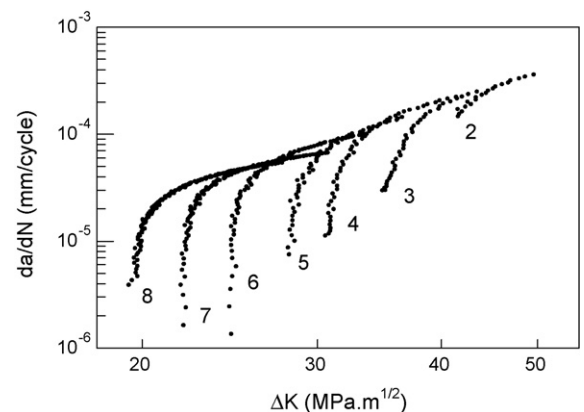


Fig. 10. Fatigue crack growth laws (cold drawn wire E7). The number next to each branch of the curve indicates the fatigue step associated with it.

by means of the finite element method together with a virtual crack extension technique on the basis of the stiffness derivative, as a function of the relative crack depth (a/D) and the crack aspect ratio (a/b).

Figs. 9 and 10 show that the steady state of fatigue crack growth is not reached, so that a sort of retardation in the crack advance produced by overstress is observed at the change from one fatigue step to another one of minor stress range, according to a mechanism similar to that of overload retardation effect as a consequence of the plastic zone next to the crack tip which, surrounded by an elastic zone of ring shape that tends to recover its original shape at unloading, is compressed in certain sense at the unloading phase. However, all fatigue crack growth branches are asymptotically convergent to a certain steady-state regime of crack growth with a Paris-like appearance, i.e., a quasi-linear plot in a double-logarithmic scale da/dN vs. ΔK , and this steady-state crack growth rate is lower in the cold drawn wire (E7, commercial prestressing steel which has undergone seven steps of cold drawing) than in the hot rolled bar (E0, base material which is not cold drawn at all), as shown in Figs. 9 and 10.

The fatigue crack propagation curves in Figs. 9 and 10 exhibit different transient stages due to the jump from one to another loading level with lower maximum load. These transient effects have been reported in the scientific literature [7] and are a consequence of the plastic zone in the vicinity of the crack tip, a phenomenon similar to the retardation effect caused by overloads during fatigue.

4. Discussion

4.1. Metallographic aspects

Figs. 11 and 12 show longitudinal metallographic sections of the hot rolled bar and the cold drawn wire, cf., [8–11]. As a summary of the effects of cold drawing on the evolution of the pearlite colony or first microstructural level [8,9], cold drawing produces a progressive orientation of the pearlite colony with

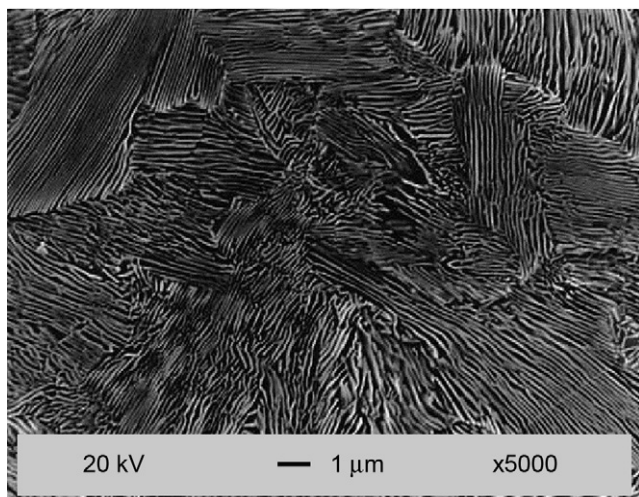


Fig. 11. Longitudinal metallographic section of the hot rolled bar (in the photograph, the horizontal side is associated with the radial direction in the bar and the vertical side corresponds to the bar axis).

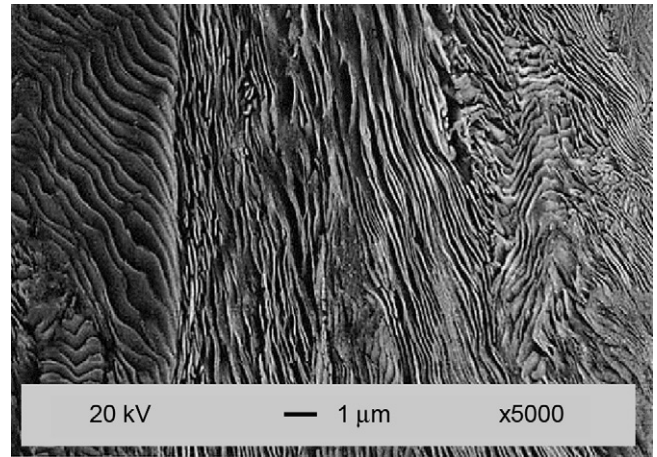


Fig. 12. Longitudinal metallographic section of the cold drawn wire (in the photograph, the horizontal side is associated with the radial direction in the wire and the vertical side corresponds to the wire axis or cold drawing direction).

its main axis approaching the axis of the wire or cold drawing direction, and a slenderising of the colony itself. In the matter of the pearlitic lamellar microstructure or second microstructural level [10,11], cold drawing produces both a decrease of inter-lamellar spacing and an orientation of the plates in the cold drawing direction.

Apart from these general trends, the metallographic analysis showed the presence of some extremely slender *pearlitic pseudocolonies* (Fig. 13) with anomalous (too large) local inter-lamellar spacing and even with pre-damage (microcracks which act as local fracture precursors) which makes them preferential fracture paths with minimum local resistance [12].

To analyse the fatigue crack growth in both steels, metallographic cuts perpendicular to the fatigue crack path plane were made in both steels, and the results are shown in Fig. 14 (hot rolled bar E0) and Fig. 15 (cold drawn wire E7). It is seen that in both cases fatigue crack growth is through the pearlitic colonies (i.e., transcolonial), with higher roughness in the cold drawn wire

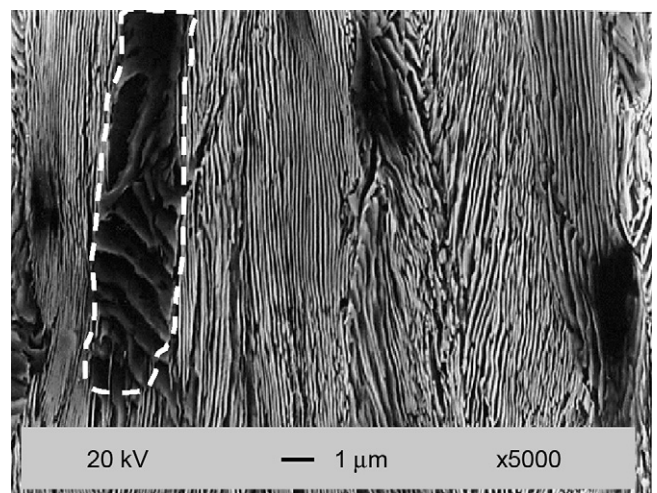


Fig. 13. Pearlitic pseudocolony in the cold drawn wire (in the photograph, the horizontal side is associated with the radial direction in the wire and the vertical side corresponds to the wire axis or cold drawing direction).

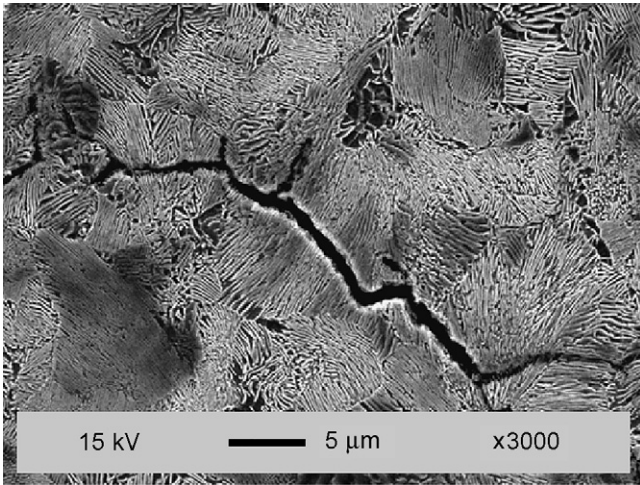


Fig. 14. Metallographic cut showing the fatigue crack growth in the hot rolled bar E0 (crack propagation from left to right).

and a growing direction changing from one to another colony. At the microscopic level, fatigue crack growth often exhibits some micro-crack branches with a deflection angle of about 45° in relation to the main crack growth direction (transverse to the wire axis). Such deflected branches could appear because fatigue cracking could follow a mechanism similar to that proposed by Miller and Smith [13] for static fracture in pearlitic microstructures. According to this mechanism of *shear cracking* in pearlite, brittle cementite lamellae fail when they are unable to undergo the big shear deformation of the more ductile ferrite.

4.2. Fatigue crack propagation

This sub-section tries to analyse the key experimental result: the fact that the crack progresses in mode I by fatigue even in the cold drawn steel, in spite of its markedly oriented pearlitic microstructure and the presence of pearlitic pseudocolonies acting as local fracture precursors. The reasons for this behaviour are three-fold:

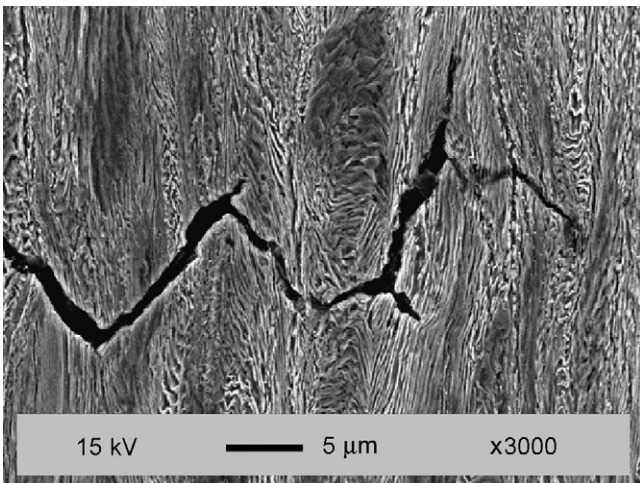


Fig. 15. Metallographic cut showing the fatigue crack growth in the cold drawn wire E7 (crack propagation from left to right).

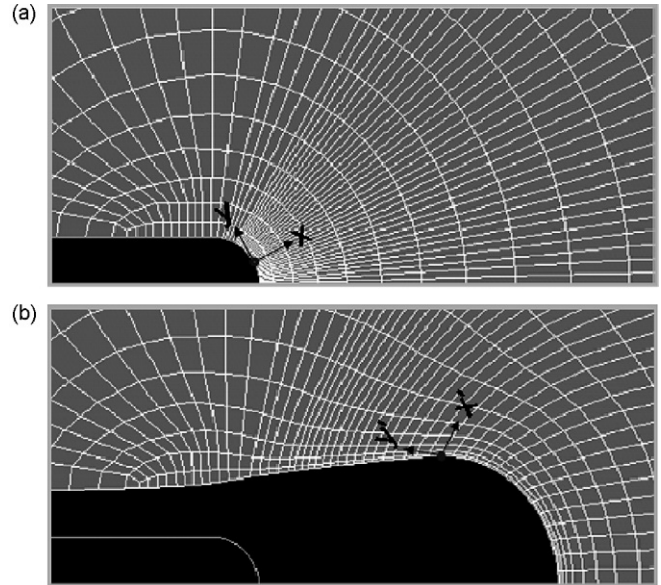


Fig. 16. Initial undeformed mesh at the crack tip (a) and deformed mesh (b) at the unloading phase after fatigue cycles, showing large deformations and rotation of axes from $x-y$ to $x'-y'$.

- (i) Crack tip blunting and large geometry changes produced by plasticity. As demonstrated in previous high-resolution numerical analyses by the finite element method [14], large strains and large geometry changes in the vicinity of the crack tip produce big rotations of axes (Fig. 16) and a clear crack tip blunting. Such a blunting is able to counter-balance the effect of the pearlitic pseudocolonies, so that posterior crack growth by fatigue in mode I after the crack has reached a pearlitic pseudocolony may be possible, as sketched in Fig. 17.
- (ii) Geometrical constraint produced by the rest of the points of the crack front that therefore tends to propagate in the original direction, as depicted in Fig. 18. This fact makes the crack deflection by fatigue more difficult.
- (iii) The orientation of the pearlitic lamellae. As a matter of fact, although in the cold drawn wire the plates are mainly oriented in the cold drawing direction and thus they are perpendicular to the crack faces, only some of them contain the crack front and tend to produce deflection, while many of them form an angle (or even are perpendicular) to the

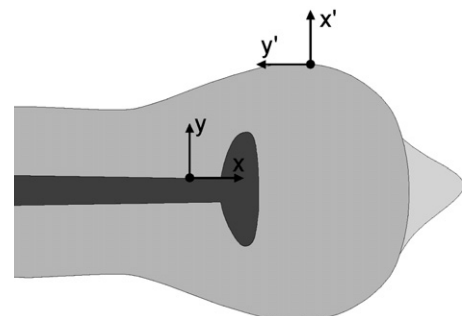


Fig. 17. Scheme showing crack tip blunting and posterior crack growth by fatigue in mode I after the crack has reached a pearlitic pseudocolony.

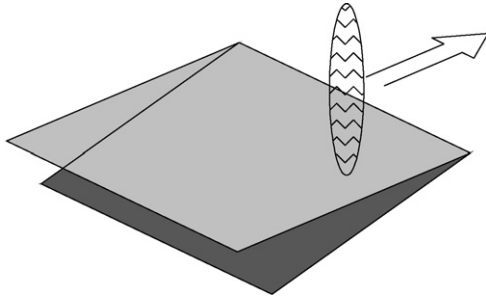


Fig. 18. Scheme showing crack growth by fatigue in mode I after the crack has reached a pearlitic pseudocolony, due to the geometrical constraint produced by the rest of the points of the crack front which therefore tends to propagate in the original direction.

crack front, in the latter case tending to produce the more difficult phenomenon of crack twinning (two symmetrical branches).

5. Conclusions

The crack front evolves by maintaining an elliptical shape during the fatigue crack growth, tending asymptotically to a stable crack front shape with constant aspect ratio a/b in the case of high-strength pearlitic steels.

In the fatigue tests with decreasing steps of constant loading a sort of retardation effect in crack growth is produced by over-stress when the change from one to another step of loading with lower stress level takes place.

By means of cold drawing a decrease in the crack growth rate is achieved, thus resulting that the manufacture process is beneficial from the points of view of damage tolerance and structural integrity of the prestressing steel wires.

The crack is able to propagate by fatigue in mode I (with no crack deflection) even in the cold drawn steel, in spite of the markedly oriented pearlitic microstructure of the material in this case and the presence of pearlitic pseudocolonies (weakest regions).

The reasons for this fact are the crack tip blunting and the large geometry changes produced by plasticity in the vicinity of

the crack tip, the constraint produced by the rest of the points of the crack front and the different orientations of the pearlitic plates (in relation to the crack line) which would tend to produce crack twinning instead of crack deflection.

Acknowledgements

The authors wish to acknowledge the financial support of their research at the University of Salamanca provided by the following institutions: Spanish Ministry for Scientific and Technological Research (MCYT-FEDER; Grant MAT2002-01831), Spanish Ministry for Education and Science (MEC; Grant BIA2005-08965), Regional Government *Junta de Castilla y León* (JCYL; Grants SA078/04 and SA067A05) and Spanish Foundation “Memoria de D. Samuel Solórzano Barruso” (Grants for Scientific and Technological Research). In addition, the authors wish to express their gratitude to TREFILERÍAS QUIJANO (Cantabria, Spain) for providing the steel used in the experimental programme.

References

- [1] A. Carpinteri, *Int. J. Fracture* 15 (1993) 21–26.
- [2] N. Couroneau, R. Royer, *Comp. Struct.* 77 (2000) 381–389.
- [3] X.B. Lin, R.A. Smith, *Int. J. Fatigue* 19 (1997) 461–469.
- [4] J. Llorca, V. Sánchez Gálvez, *Eng. Fracture Mech.* 26 (1987) 869–882.
- [5] J. Toribio, M. Toledano, *Constr. Build. Mater.* 14 (2000) 47–53.
- [6] M.A. Astiz, *Int. J. Fracture* 31 (1986) 105–124.
- [7] S.Ya. Yarema, *Test Method for Determination of Crack Growth Rate and Crack Extension Resistance Under Cyclic Loading*, Academy of Sciences of Ukraine, National Karpenko Physico-Mechanical Institute, Lviv, 1994.
- [8] J. Toribio, E. Ovejero, *Mater. Sci. Eng. A234–236* (1997) 579–582.
- [9] J. Toribio, E. Ovejero, *J. Mater. Sci. Lett.* 17 (1998) 1037–1040.
- [10] J. Toribio, E. Ovejero, *Scripta Mater.* 39 (1998) 323–328.
- [11] J. Toribio, E. Ovejero, *Mech. Time-Dependent Mater.* 1 (1998) 307–319.
- [12] J. Toribio, E. Ovejero, M. Toledano, *Int. J. Fracture* 87 (1997) L83–L88.
- [13] L.E. Miller, G.C. Smith, *J. Iron Steel Inst.* 208 (1970) 998–1005.
- [14] J. Toribio, V. Kharin, *Advances in Fatigue Crack Closure Measurement and Analysis*. ASTM STP 1343, American Society for Testing and Materials, PA, USA, 1999, pp. 440–458.